CONF-900268--1

Heat Capacities of Solid Polymers

(The Advanced THermal Analysis System, *ATHAS*)

DE90 007130

Bernhard Wunderlich

Department of Chemistry, The University of Tennessee
Knoxville, TN 37996-1600
and
Division of Chemistry, Oak Ridge National Laboratory
Oak Ridge, TN, 37831-6197

Abstract

The thermal properties of solid, linear macromolecules are accessible through heat capacity measurements from about 10 K to the glass transition. By measuring and collecting data on over 150 polymers, a data bank was established and used as a base for detailed correlation with an approximate frequency spectrum for the polymers. Besides assessment of the entropy at zero kelvin of disordered polymers, this heat capacity knowledge has helped in the elucidation of partial phase transitions and conformationally disordered crystal phases. A link has also been established to measurements of mobility through solid state nuclear magnetic resonance. Most recently heat capacity measurements have been linked to full dynamic simulations of crystal segments of 1900 chain atoms. Questions of disorder and anharmonicity can thus be analyzed. The work is summarized as the Advanced THermal Analysis System, *ATHAS*.

DISCLAIMER

This report was prepared as an account of work sponsored by an agency of the United States Government. Neither the United States Government nor any agency thereof, nor any of their employees, makes any warranty, express or implied, or assumes any legal liability or responsibility for the accuracy, completeness, or usefulness of any information, apparatus, product, or process disclosed, or represents that its use would not infringe privately owned rights. Reference herein to any specific commercial product, process, or service by trade name, trademark, manufacturer, or otherwise does not necessarily constitute or imply its endorsement, recommendation, or favoring by the United States Government or any agency thereof. The views and opinions of authors expressed herein do not necessarily state or reflect those of the United States Government or any agency thereof.

"The submitted manuscript has been authored by a contractor of the U.S. Government under contract No. DE-AC05-84OR21400. Accordingly, the U.S. Government retains a nonexclusive, royalty-free license to publish or reproduce the published form of this contribution, or allow others to do so, for U.S. Government purposes."

MASTER

DISTRIBUTION OF THIS DOCUMENT IS UNLIMITED

In order to describe the heat capacities of linear macromolecules the Advanced *THermal Analysis System* was developed.[1] Several steps are necessary before an approximation of the heat capacity in terms of its vibrational spectrum can be made. First, one finds that linear macromolecules do not normally crystallize completely, they are usually *semicrystalline*. The restriction to partial crystallization is caused by kinetic hindrance to full extension of the molecular chains which, in the amorphous phase, are randomly coiled and entangled. Furthermore, in case the molecular structure is not sufficiently regular, the crystallinity may be further reduced, or even completely absent so that the molecules remain *amorphous* at all temperatures. Copolymers offer typical examples.

The first step in the analysis must thus be to establish the crystallinity dependence of the heat capacity. Polyethylene, the most analyzed polymer, is treated first. The fact that polyethylene, $[(CH_2-)_x]$, is semicrystalline implies that the sample is metastable, i.e. not in equilibrium. Thermodynamics requires that a one-component system like polyethylene can have only two phases in equilibrium at the melting temperature (phase rule).

One way to establish the *weight-fraction crystallinity*, w_c, is from density measurements (dilatometry). The equation is given as Fig. 1. A similar equation can be derived for the *volume-fraction crystallinity*, v_c. Plotting the measured heat capacities of samples with different crystallinity often results in a linear relationship. Such plots allow the extrapolation to crystallinity zero, to find the heat capacity of the amorphous sample, and to crystallinity 1.0, to find the heat capacity of the completely crystalline sample, even if these limiting cases are not experimentally available.

$$w_c = \left(\frac{\varrho_c}{\varrho}\right)\left(\frac{\varrho_c - \varrho_a}{\varrho - \varrho_a}\right)$$

c = crystalline w_c = crystallinity
a = amorphous ϱ = density

Fig. 1 Weight fraction crystallinity.

Figures 2 and 3 illustrate the experimental heat capacities for polyethylene. A number of other polymers are described in the *ATHAS* Data Bank.[2].

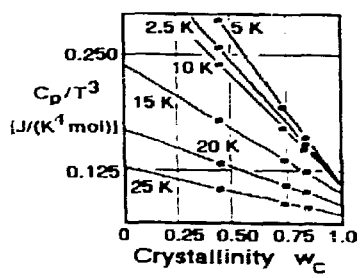

Fig. 2. Crystallinity dependence of the heat capacity of polyethylene at low temperature.

The curves in Fig. 2 show linear crystallinity dependence. For the fully crystalline sample (w_c = 1.0) there is a T^3 temperature dependence of the heat capacity up to 10 K (single point in the graph), as is required for the low-temperature limit of a 3-dimensional Debye function.[3] This T^3-dependence is not very extended, at 15 K it is already lost. This trend of heat capacity is caused by an adherence to a quadratic increase in number of vibrators of increasing frequencies, ν. This trend is adhered to for increasingly shorter ranges of frequency in the sequence diamond, graphite, polyethylene.

The amorphous polyethylene (w_c = 0) seems, in contrast, never to reach a T^3 temperature dependence of the heat capacity. Note that the curves of the figure do not even change monotonously with temperature.

As the temperature is raised, the crystallinity dependence of the heat capacity becomes less, and is only a few percent between 50 to 200 K. In this temperature range the heat capacity is largely independent of the physical structure. Glass and crystal have almost the same heat capacity. This is followed again by a steeper increase in heat capacity as the amorphous polymer undergoes the *glass transition* at about 240 K. Figure 3 shows the crystallinity dependence just above the glass transition. It is of interest to note that the fully amorphous value from this graph agrees well with the extrapolation of the heat capacity of the liquid from above the melting temperature (414.6 K) which leads to 28.5 J/(K mol).

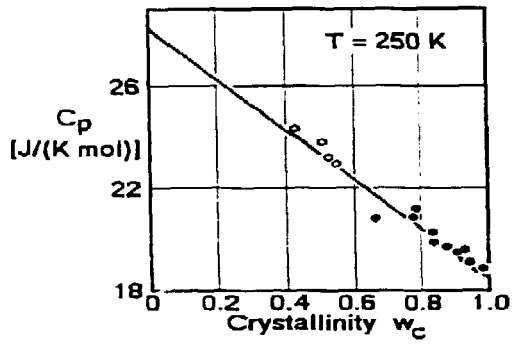

Fig. 3. Crystallinity dependence of the heat capacity of polyethylene at 250 K.

Finally, Fig. 4 shows that above about 260 K, melting of small, metastable crystals causes an abnormal, nonlinear deviations in the heat capacity versus crystallinity plot. The measured data are indicated by the heavy lines in the figure. The thin lines indicate how continued additivity would look. The points for amorphous polyethylene at the left of the figure represent the melt and agree with the extrapolation of the measured heat capacities from the melt. All heat capacity contributions above the thin lines must thus be assigned to nonequilibrium melting.

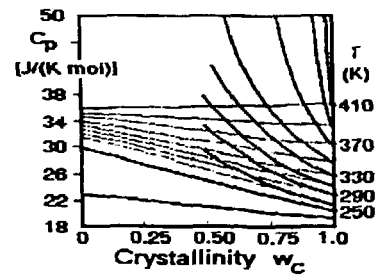

Fig. 4. Crystallinity dependence of the heat capacity of polyethylene in the melting region of small crystals.

The data in Figs. 2-4 permit now an extrapolation of the measured heat capacities to the completely crystalline and to the fully amorphous states. The results of such extrapolations are shown in Fig. 5. The heat capacities in Fig. 5 are characterized for the crystalline sample by a T^3 dependence to 10 K. This is followed by a change to a linear temperature dependence up to about 200 K. Such temperature dependence of heat capacity fits a one-dimensional Debye function well.[3] Then, one notices a slowing of the increase of the crystalline heat capacity with temperature at about 200 to 250 K, to show a renewed increase above 300 K, to reach (close to the melting temperature) values equal to and higher than the heat capacity of molten polyethylene. The heat

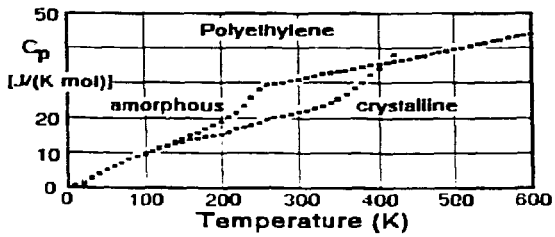

Fig. 5. Heat capacities of crystalline and amorphous polyethylene, obtained by extrapolation to complete and zero crys-tallinity.

capacity of the glassy polyethylene shows large deviations from the heat capacity of the crystal at low temperature. At these temperatures the absolute value of the heat capacity is so small that it does not show up in the figure. After a long range of almost equal heat capacities of crystal and glass, the glass transition is obvious at about 240 K. In the melt, the heat capacity is linear over a very wide temperature region.

This quite complicated temperature dependence of the macroscopic heat capacity must now be explained by a microscopic model of thermal motion. Neither a single Einstein function [4], nor any of the Debye functions [3] have any resemblance to the experimental data. It helps in the analysis that the vibration spectrum of crystalline polyethylene is known in detail from calculations using force constants derived from infrared and Raman spectroscopy.[2] Such spectrum is shown in Fig. 6. Using a different Einstein function for each vibration [4], one can compute the heat capacity by adding the contributions of all the various frequencies. The heat capacity of the crystalline polyethylene shown in Fig. 5 can be reproduced above 50 K by these data within experimental error.

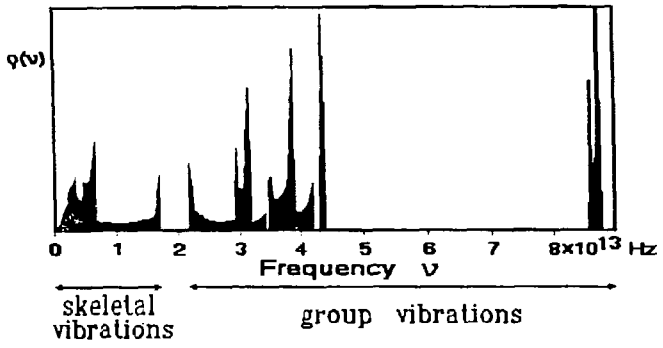

Fig. 6. Vibrations of crystalline polyethylene.

Below 50 K the experimental data show increasing deviations, an indication that the computation of the low-frequency, skeletal vibrations cannot be carried out correctly at present.[5]

With the knowledge of heat capacity *and* frequency spectrum, one can discuss the actual motion of the molecules in the solid state. Looking at the frequency spectrum of 6, one can distinguish three separate frequency regions. The first region goes up to approximately 2×10^{13} Hz. One finds vibrations that account for two degrees of freedom in this range. The motion involved in these vibrations can be visualized as a torsional and an accordion-like motion of the CH_2-backbone, as illustrated in sketches 1 and 2 of Fig. 7. The torsion can be thought of as a motion that results from twisting one end of the chain against the other about the molecular axis. The accordion-like motion of the chain arises from the bending motion of the C-C-C-bonds on compression of the chain, followed by extension. These two low frequency motions will be called the *skeletal vibrations*. Their frequencies are such that they contribute mainly to the increase in heat capacity from 0 to 200 K.

The next group of frequencies starts to contribute to the heat capacity at a somewhat higher temperature. The gap in the frequency distribution is responsible for the levelling of the heat capacity between 200 and 250 K. The absolute level of the plateau is of the proper order of magnitude for two degrees of freedom, i.e. about 16-17 J/(K mol) or $2R$.

All motions of higher frequency will now be called *group vibrations*, because these vibrations involve oscillations of relatively isolated groupings of atoms

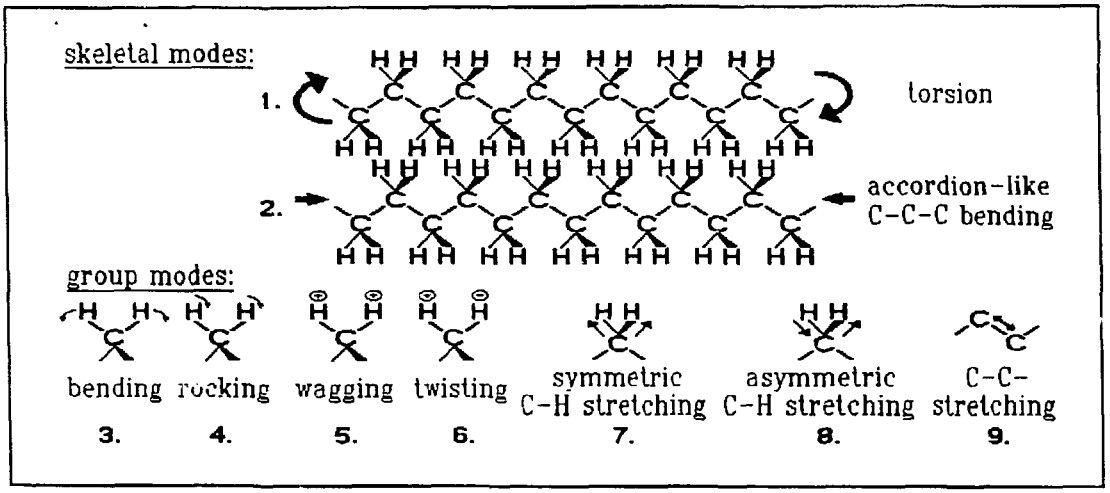

Fig. 7. Approximate vibrational modes in crystalline polyethylene.

along the backbone chain. In the first set of group vibrations, between 2 and 5×10^{13} Hz, one finds five degrees of freedom. These oscillations involve mainly the bending of the C-H-bond and the C-C-stretching vibration. The sketches 3-6 in Fig. 7 illustrate the approximate C-H-motions of the bending vibrations. The first type of motion involves the symmetrical *bending* of the hydrogens (3). The bending motion is indicated by the arrows. The next type of oscillation is the *rocking* motion (4). In this case both hydrogens move in the same direction and rock the chain back and forth. The third type of motion in this group, listed as number 5, is the *wagging* motion. One can think of it as a motion in which the two hydrogens come out of the plane of the paper and then go back behind the plane of the paper. The *twisting* motion (6), finally, is the asymmetric counterpart of the wagging motions, i.e. one hydrogen comes out of the plane of the paper while the other goes back behind the plane of the paper. In addition to these bending motions of C-H, there is a motion in the same frequency region that is involved with the *stretching* of the bond between two adjacent carbon atoms (sketch 9). This stretching of a C-C-bond has a much higher frequency than the torsion and bending involved in the skeletal modes. Although it looks like a skeletal vibration, it is not coupled sufficiently along the chain to result in a broad frequency distribution. These five vibrations are the ones responsible for the renewed increase of the heat capacity starting at about 300 K. Below 200 K their contributions to the heat capacity are small.

Finally, the CH_2-groups have two more degrees of freedom, the ones that contribute to the very high frequencies above 8×10^{13} Hz. These are the *C-H-stretching* vibrations. There is a symmetric and an asymmetric one, as shown in the bottom sketches 7 and 8 of Fig. 7. These frequencies are so high, that at 400 K their contribution to the heat capacity is still small. Summing all these contributions to the heat capacity of polyethylene, one finds that up to about 300 K mainly the skeletal vibrations contribute to the heat capacity, above 300 K, increasing contributions come from the group vibrations in the $2\text{-}5 \times 10^{13}$ Hz region and, if one could have solid polyethylene at about 700-800 K, then one would get the additional contributions from the C-H-stretching vibrations, but polyethylene crystals melt before these vibrations are excited significantly. The total of nine vibrations possible for the three atoms of the CH_2-unit, would, when fully excited, lead to a heat capacity of 75 J/(K

mol). At the melting temperature, only half of these vibrations are excited, C_v is about 38 J/(K mol).

Only for few other polymers is so much information on the vibrational frequency spectrum available.[5] In case the vibrational spectrum is not available, one may want to try to calculate vibrational spectra from heat capacities, a process called an *inversion* of the heat capacity. Because the heat capacities are not very sensitive to the detailed frequency spectrum, only a relatively coarse approximation of the spectrum can be obtained in this way. It is not even certain, that the inversion leads mathematically to a unique frequency spectrum.

The analysis of heat capacity of a given homopolymer starts, thus, with the evaluation of the experimental crystalline and amorphous heat capacities over as wide a temperature range as possible. For amorphous polymers the glassy and liquid heat capacities are directly measurable. For crystallizing polymers, the crystalline and amorphous heat capacities may have to be extrapolated, as illustrated on the polyethylene example in Figs. 2-4. Only in rare cases are almost completely crystalline polymers samples available (as for example, for polyethylene, polytetrafluoroethylene, polymeric selenium, and polyoxymethylene).

Vibration Type	Θ_E, Θ_L, Θ_U (K)	N
CH2 symm. stretch	4284.7	1.00
CH2 asym. stretch	4168.2	1.00
CH2 bending	2104.5	1.00
CH2 wagging	2018.6	1.00
CH2 twisting	1921.9	1.00
CH2 rocking	1524.7	0.20
	1707.2	0.24
	1524.7-1707.2	0.56
C-O stretching	1385.1	0.22
	1892.1	0.11
	1385.1-1632.1	0.67
	1304.6	1.00
chain bending	869.7	1.00
	655.0	0.29
	359.7- 440.2	0.29
	359.7- 655.0	0.48

Fig. 8. List of group vibrations of poly(oxymethylene).

Vibration Type	Θ_E, Θ_L, Θ_U (K)	N
CH_2 symm. stretch	4097.7	1.00
CH_2 asym. stretch	4148.1	1.00
CH_2 bending	2074.7	1.00
CH_2 wagging	1698.3-1976.6	0.65
	1976.6	0.35
CH_2 twisting + CH_2 rocking	1689.6-1874.3	0.48
	1874.3	0.52
C-C stretching	1977.6-1697.5	0.94
	1377.8-1525.4	0.35
	1525.4	0.31
CH_2 twisting + CH_2 rocking	1494.1	0.04
	1038.0-1494.1	0.59
	1079.1	0.37

Fig. 9. List of group vibrations of polyethylene.

Next, the experimental heat capacity at constant pressure, C_p, is converted to C_v using standard thermodynamic relationships or approximations.[6] The total experimental C_v is then separated into the part due to the group vibrations and the part due to the skeletal vibrations. The heat capacity due to the group vibrations is calculated from an approximate spectrum of the group vibrations as listed for the polyoxymethylene $[(CH_2-O-)_x]$ and the polyethylene in Figs. 8 and 9.[7] The CH_2-bending and -stretching vibrations are similar for both polymers. To increase the precision, some of the group

$$(1)\quad C_{box} = NR\frac{\Theta_U}{(\Theta_U - \Theta_L)}\left[D_1\left(\frac{\Theta_U}{T}\right) - \left(\frac{\Theta_U}{\Theta_L}\right)D_1\left(\frac{\Theta_L}{T}\right)\right]$$

$$(2)\quad C_v(\text{skeletal}) = C_v(\text{total}) - C_v(\text{group vibrations})$$

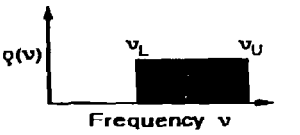

Fig. 10. Equations for the computation of heat capacity from a box distribution of vibrations.

vibrations that spread over a wider frequency ranges were approximated by *box-distributions*. The heat capacity contribution is computed with the help of two one-dimensional Debye functions [3], as represented by Eq. (1) in Fig. 10. The lower frequency limit is given by θ_L, the upper one by θ_U. The figure on the right shows the corresponding frequency distribution. Subtracting of all heat capacity contributions of the group vibrations from the measured C_V yields the experimental, skeletal heat capacity contribution [Eq. (2)].

The last step in the *ATHAS* analysis is to asses the skeletal heat capacity. The skeletal vibrations are coupled in such a way that their distribution

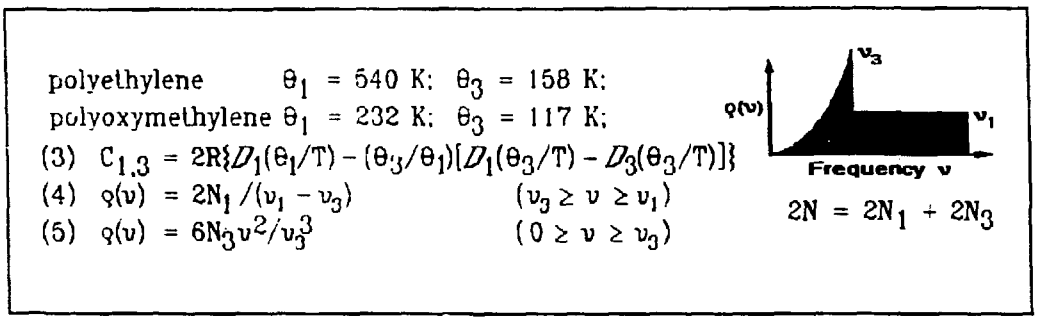

Fig. 11. Approximation of the skeletal vibrations of a polymer.[8]

stretches to zero frequency (*acoustical vibrations*). In the lowest frequency region one must, in addition, also consider that the vibrations couple *intermolecularly* because the wavelengths of the vibrations become larger than the molecular anisotropy caused by the chain structure. As a result, the detailed molecular arrangement is of little consequence at the lowest frequencies. A three-dimensional Debye function, derived for an isotropic solid [3] should apply in this frequency region. For diamond such function was shown to apply up to about 2×10^{13} Hz. Only above that frequency did the detailed atomic structure become of importance for the spectrum. For graphite, this limit of the applicability of the three-dimensional Debye function occurred already at 0.5×10^{13} Hz. For linear polyethylene, finally, the spectrum in Fig. 6 limits the ν^2-dependence to less than 0.2×10^{13} Hz. To approximate the skeletal vibrations of linear macromolecules one should thus start out at low frequency with a three-dimensional Debye function and then switch to a one-dimensional Debye function. Such an approach was suggested by Tarasov.[8] The skeletal vibration frequencies were separated into two groups, the intermolecular group between zero and ν_3, (characterized by a three-dimensional θ-temperature, θ_3), and an intramolecular group between ν_3 and ν_1 (characterized by a one-dimensional θ-temperature, θ_1). Equation (3) in Fig. 11 shows the needed computation and reveals that by assuming that the number of vibrators in the intermolecular part is θ_3/θ_1, one has only two adjustable parameters in the equation. The distribution is fitted to the experimental heat capacities at low temperatures, to get θ_3, and at higher temperatures, to get θ_1. Computer programs for the fitting over the whole temperature region are available.[9] For polyethylene and polyoxymethylene the best fit was obtained for the θ-temperatures shown in Fig. 11. These values are not too different from the end of the ν^2-dependence of the actual frequency spectrum. A more detailed discussion of the correspondence of frequency spectrum computed and fitted to heat capacity is given in Ref. [5].

With the table of group vibration frequencies, the two Θ-temperatures and the number of skeletal vibrators, N, it is now possible to calculate C_V, and

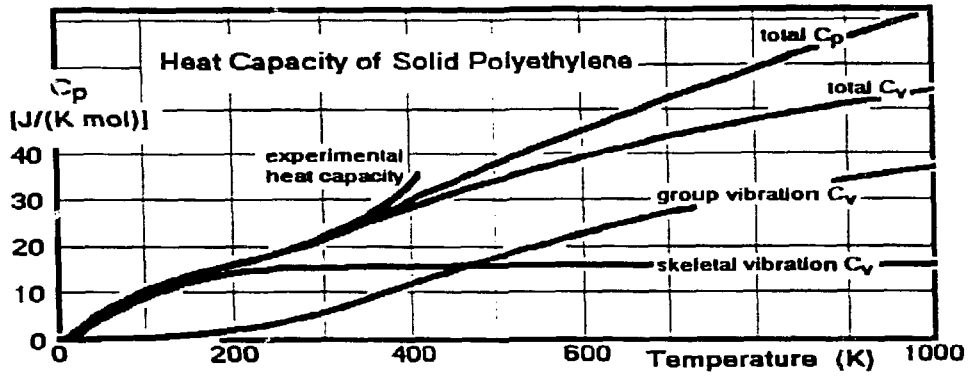

Fig. 12. Computed heat capacities of polyethylene using *ATHAS*.

with help of the expressions for $C_p - C_V$, also C_p. Figure 12 shows such calculation for polyethylene (top diagram) and for a whole series of aliphatic polyoxides (bottom diagram). In the top diagram the contribution of the skeletal vibrations and the contribution of the group vibrations are shown separately. The experimental data, finally show the good experimental fit to heat capacity at constant pressure, C_p.

Since group vibrations are not affected much by their chemical environment, it becomes now possible from the table in Fig. 8 not only to compute the heat capacity of polyoxymethylene, but also of all other aliphatic polyoxides, as

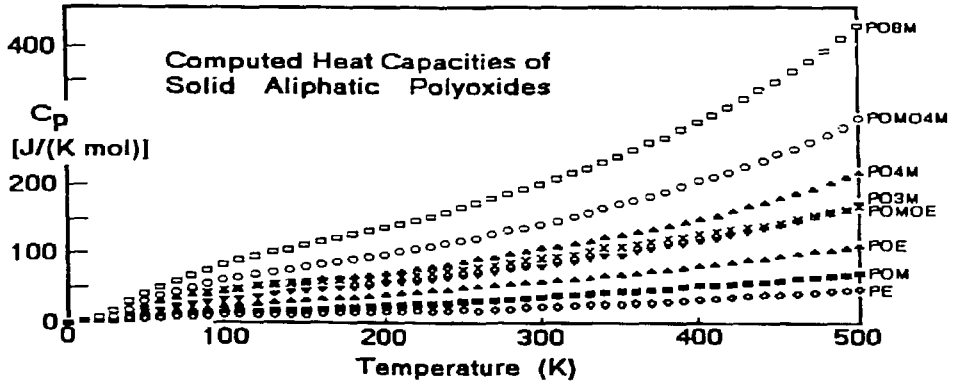

Fig. 13. Heat capacities of the aliphatic polyoxides computed by the *ATHAS*. For abbreviations see the listing in the text.

shown in the Fig. 13. The abbreviations are to be translated as follows:

PO8M	=	Polyoxyoctamethylene $[O-(CH_2-)_8]_x$
POMO4M	=	Polyoxymethyleneoxytetramethylene $[O-CH_2-O-(CH_2-)_4]_x$
PO4M	=	Polyoxytetramethylene $[O-(CH_2-)_4]_x$

PO3M = Polyoxytrimethylene $[O-(CH_2-)_3]_x$
POMOE = Polyoxymethyleneoxyethylene $[O-CH_2-O-(CH_2-)_2]_x$
POE = Polyoxyethylene $[O-(CH_2-)_2]_x$
POM = Polyoxymethylene $[O-CH_2-]_x$
PE = Polyethylene (polymethylene) $[CH_2-]_x$

The more detailed analysis of the heat capacities of the solid, aliphatic polyoxides is summarized in Fig. 14. The top graph shows the deviations of the

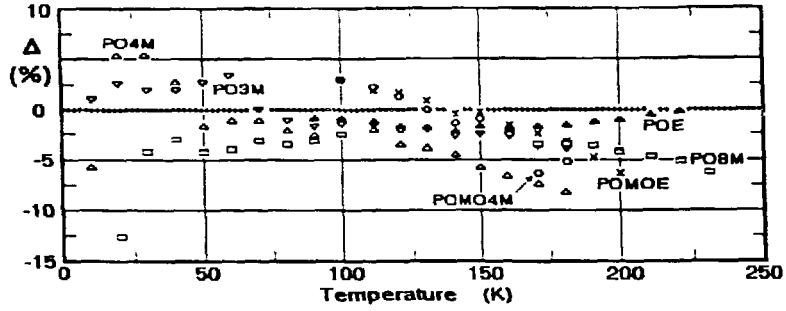

Fig. 14. Deviation of C_p of the polyoxides from the experiment.

calculations from the experiment as exressed by the equation:

$$\Delta = [C_p(\text{computed}) - C_p(\text{experimental})]/C_p(\text{experimental})]$$

Figures 15 and 16 indicate that the Θ_1 and Θ_3 values are changing continuously with chemical composition. It is thus possible to estimate Θ_1 and Θ_3 for intermediate compositions, and to compute heat capacities of unknown poly

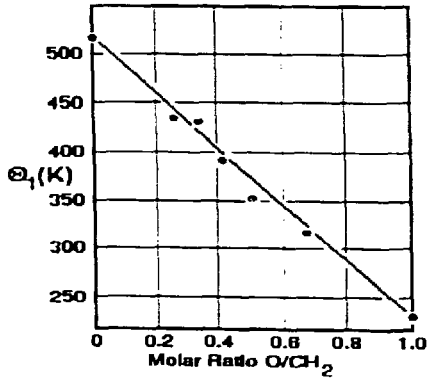

Fig. 15. Theta temperatures of polyoxides

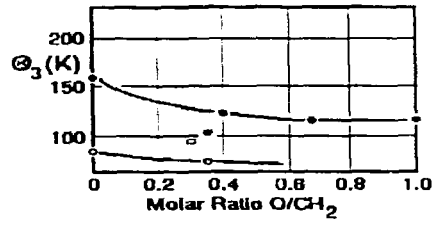

Fig. 16. Theta temperatures of polyoxides.

oxides or copolymers of different monomers without reference to measurement.

Similar analyses were accomplished for more than 150 macromolecules. The data on N, Θ_1 and Θ_3 together with the ranges of experimental C_p-data are collected in the *ATHAS* Data Bank.[2] The precision of these computed heat capacities is in general better than ±5%.

The strict additivity of the heat capacity contributions of the group vibrations and the continuous change in Θ_1 with chemical composition led to the

development of *addition schemes* for heat capacities. As long as the contributions of the backbone groupings that make up the polymer are known empirically, it is reasonable to estimate the heat capacity of unknown polymers and copolymer from these contributions. Detailed tables can be found in Refs. [10] and [11].

The heat capacities of liquids are much more difficult to understand.[9] The motion involves now also large-amplitude rotations and translations. Since in the liquid state polymers are usually in equilibrium, measurements are more reproducible, as is shown on the example of polyoxymethylene in Fig. 17.[12]

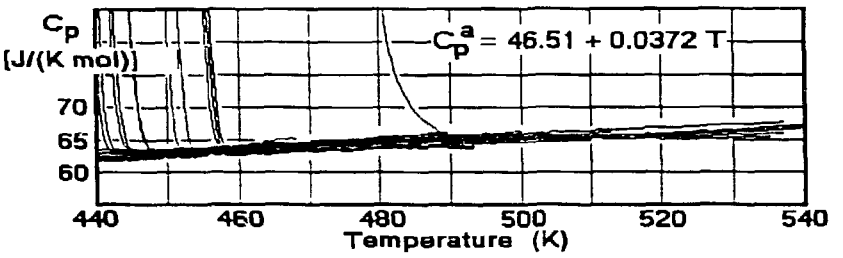

Fig. 17. Direct print of 36 heat capacity measurements on liquid polyoxymethylene.[13]

The graph is a direct copy of 36 runs of differently treated polyoxymethylenes. The almost vertical approach of some of the curves to the liquid heat capacity is caused by the end of melting of crystallized samples.

The addition scheme helps, next, to connect larger bodies of data. Figure 18 shows the experimental data for the liquids for the same series of polyoxides as shown in Fig. 13 for the solid state. The equation in the top of the graph represents all the thin lines, the thick lines represent the experimental data. The equation for C_p^a was arrived at by least square fitting of all experiments. Again, the *ATAS* Data Bank [3] gives a listing for available data on other polymers.

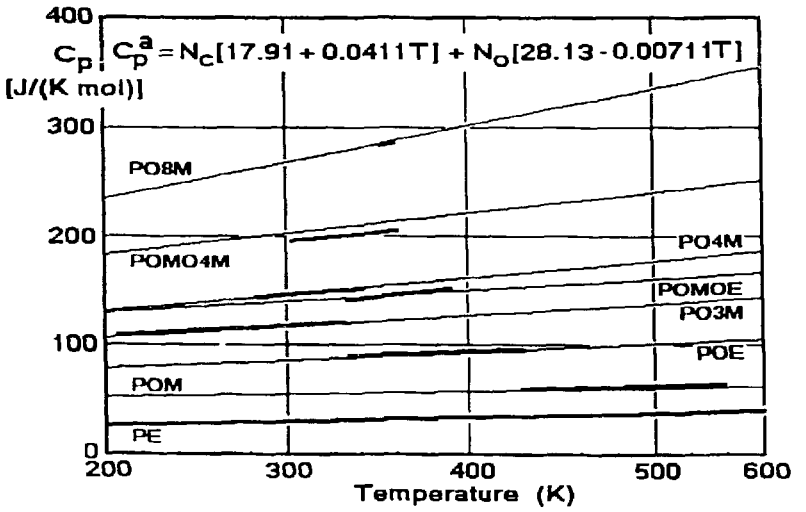

Fig. 18. Heat capacities of liquid polyoxides.

The application of the *ATHAS* has produced not only a large volume of heat capacity data on solid and liquid homopolymers, helpful in the determination

of the integral thermodynamic functions, but it is also of help in the separation of nonequilibrium enthalpy and heat capacity effects. Figures 19 and 20 show two typical examples. At the top, the measured and computed heat

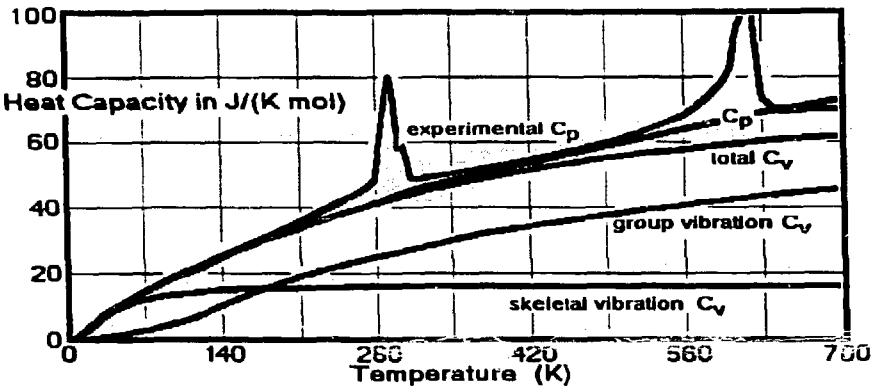

Fig. 19. The heat capacity of polytetrafluoroethylene.

capacities of polytetrafluoroethylene are reproduced.[14] As in the case of the polyoxides, it is also possible to predict heat capacities of all less fluorinated polyethylenes.[15] The measured sample was almost completely crystalline, but it is obvious from the graph that there are two rather broad endotherms superimposed on the heat capacity curves. The room-temperature transition is particularly broad. It represents a crystal-to-condis-crystal transition.[16] Without the computed heat capacity as a base line, it is impossible to separate the heat of transition quantitatively from the heat capacity.

Figure 20 is even more complicated. In this case the macromolecule is the random copolymer poly(oxybenzoate-*co*-oxynaphthoate),[17] a polymer, designed

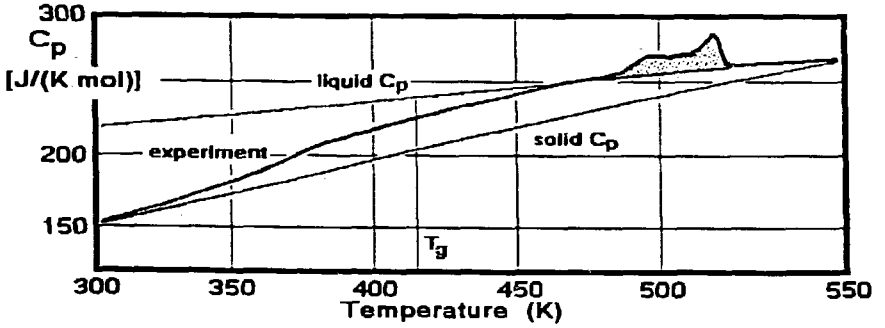

Fig. 20. Heat capacity of a liquid crystalline copolyester.

to be used in composites. The graph shows a rather small endotherm and a rather broad, possibly two-stage glass transition that stretches over more than 100 K. Without precise computation of the liquid and solid heat capacities, it would not have been possible to identify the glass transition and provide important characteristics for the practical application of the polymer.

To describe *heat capacities of copolymers*, it is naturally impossible to measure each and every composition. The trend of the heat capacities in the solid as well as the liquid states to be additive with respect to composition, allows to make estimates of the heat capacities of the copolymers (see also the *ATHAS* empirical addition schemes, Refs. [10] and [11]).

Figure 21 shows the additivity of the heat capacities of poly(styrene-co-butadiene). These measurements were done many years ago by adiabatic calorimetry and it was possible later to derive the heat capacity of the copolymers from their molar composition and the heat capacities of the constituent homopolymers.[18] As indicated in the equation, it is also possible to add more than two components. A conspicuous feature of the polybutadiene and the copolymer heat capacities is the increase of the temperature of the glass transition with styrene composition. The glass transition of pure polystyrene occurs at 373 K. Comparing now the measured heat capacity with the heat capacity calculated from the addition scheme, one finds an error between 0 and 4% from 10 K to the beginning of the glass transition. But even above the glass transition temperature the additivity works well. The errors are less than 5%. Note that for the addition scheme the contributions of *both* components, the butadiene as well as the styrene, must be taken as their liquid heat capacities as soon as the copolymer glass transition temperature has been exceeded. Position and breadth of the glass transition has to be predicted from other considerations.

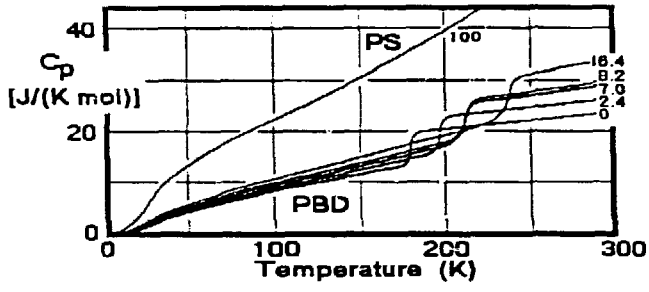

Fig. 21. Heat capacities of various poly(styrene-*co*-1-4-butadiene)s. The composition is listed in mol-%.

To conclude the treatment of heat capacities, there is a brief mention of the heat capacity of liquid selenium. The heat capacity for many liquid, linear macromolecules increases linearly with temperature, despite the fact that one expects an exponential increase in C_V from the vibrational contributions of the C-H-bending and -stretching vibrations. To understand this observation, one has to remember that a decreasing heat capacity contribution with temperature results in the framework of the hole theory from

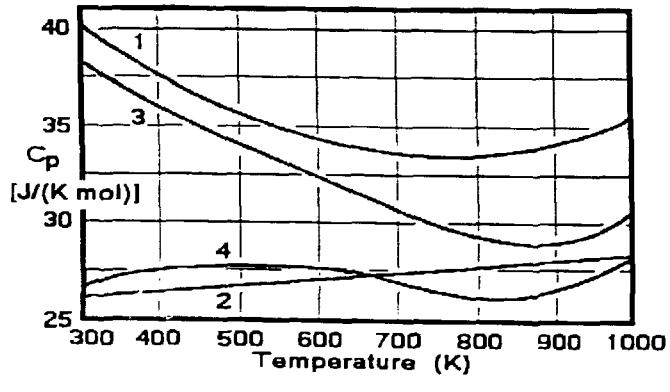

Fig. 22. Heat capacity contributions for liquid selenium.

the holes in a liquid. An approximate calculation of the hole contribution to the heat capacity can be made using a two energy state model. A maximum in heat capacity occurs close to the glass transition temperature. The subsequent decrease seems to be able to compensate much of the vibrational increase in heat capacity for a considerable temperature range.[19] Looking now at the heat capacity of the monatomic, liquid selenium, one finds that there are no group vibrations to produce the exponential increase in C_p and, indeed, the heat capacity of the liquid Se decreases with temperature. The decrease in C_p is nonlinear, and at high temperature, C_p increases again. These changes in heat capacity with temperature are specific to Se, and an explanation is given in the graph at the bottom of Fig. 22.[20] Curve 1 represents the experimental data. Curve 2, the vibrational contributions as derived from the crystalline vibrational spectrum. The difference between curves 1 and 3 represents the special contribution to the heat capacity that arises from the ring-chain equilibrium, i.e. from a chemical reaction. The melt of selenium consists of very long macromolecules $(Se-)_x$ and rings of mainly Se_8 composition. The two components are in a temperature-dependent equilibrium and the difference between curves 1 and 3 is an estimate of the heat of reaction per kelvin of temperature increase for this process.[20] Finally, the difference between curves 3 and 4 is an estimate of the heat capacity due to the hole equilibrium. It decreases with temperature, as expected. The agreement between curves 4 and 2 is, finally, a measure of the quality of the model that was chosen for the interpretation of the change of heat capacity with temperature.

From the addition scheme of heat capacities[10,11] it is possible to deduce the heat capacity of of another, hypothetical, monatomic polymeric chain, namely $(O-)_x$. Its heat capacity is estimated by subtracting the $(CH_2-)_a$ contribution to the heat capacity from the total heat capacity of the polyoxides which are shown in the bottom graph of Fig. 22. As in the Se heat capacities, the heat capacity of $(O-)_x$ decreases with temperature. This decreasing heat capacity with temperature increase is also obvious from the summary equation of Fig. 18

Figure 23 illustrates the ultimate result of thermal analysis of two crystalline linear macromolecules.[21] Two isomers of 1,4-polybutadiene are analyzed. All data were extrapolated to 100% crystal-

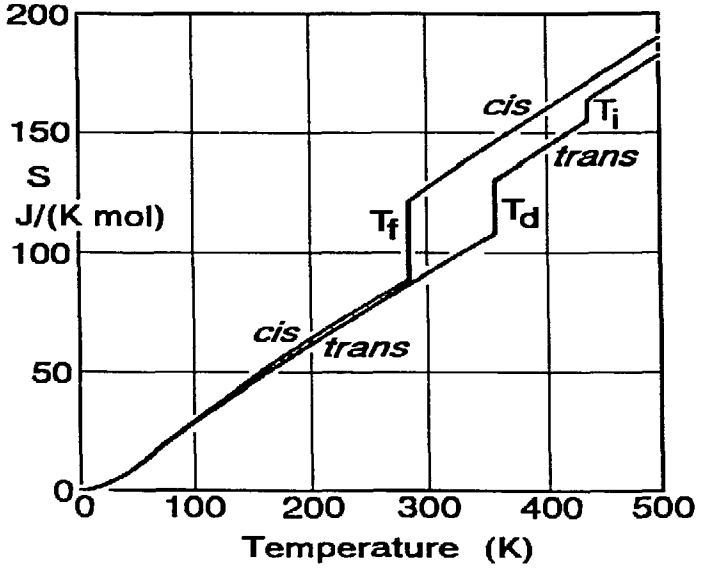

Fig. 23. Entropy of cis- and trans-1,4-polybutadiene, as computed from the heat capacity, by integration of C_p/T from 0 K and addition of the appropriate entropies of transition.

linity and equilibrium. Then the entropy was computed, adding the transition entropies at the expected equilibrium temperatures. Clearly, the *trans*-isomer melts in two steps, while the *cis*-isomer melts in a single step. The intermediate phase of the *trans*-isomer, the mesophase, has conformational disorder and represents a new class of crystals (condis crystals) that was discovered by quantitative thermal analysis.[16, 22] While the largest contribution to the entropy is caused by the vibrations, the transitions cause abrupt changes. In the condis crystalline state of *trans*-1,4-polybutadiene conformational disorder and motion is introduced without loss of positional and orientational order. Melting to the isotropic state is only comlete after the second transition at T_i.

A final topic concerns the influence of the crystalline segments on the amorphous portions of the molecules.

Advanced thermal analysis adds also one more dimension to the analysis of the glass transition. It permits the quantitative evaluation of ΔC_p, the change in heat capacity at the glass transition. An empirical rule which suggested that ΔC_p is about 11 J/(K mol) for small mobile units (beads) and two or three times as much for larger beads could be verified for many macromolecules.[2] Based on this empirical observation one can use ΔC_p as a materials characterization parameter. Mesophases as identified in Fig. 23 show often a similar ΔC_p for every mobile bead that loses its mobility at the corresponding glass transition.[16]

The behavior of block copolymers and the discovery of *rigid amorphous polymers*, the amorphous portions of molecules that are restrained by crystals, are discussed as a final application of *ATHAS*. In block copolymers of decreasing compatibility there is no way to separate the different blocks into macroscopic, separate homopolymer phases. The parts of the molecules can, at best, separate into microphases* since all junction points between the different blocks must be located at the interface. The phase size is then dependent on both concentration *and* chain length of the respective components. Because of the small size of the phases and attachment between the components, an *asymmetric broadening* of the glass transitions of the components is observed. A detailed analysis of the block copolymer poly(styrene-*co*-α-methylstyrene) is, for example, given in Ref. [23]. With decreasing block size the low temperature glass transition of the polystyrene blocks is increasingly broadened towards the higher glass transition of the poly(α-methylstyrene) blocks. At the glass transition of the polystyrene blocks the interface remains glassy due to the

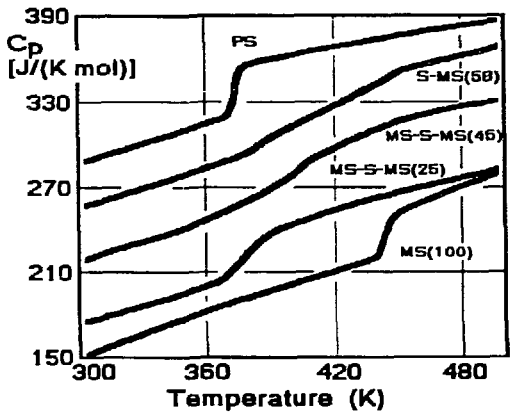

Fig. 24. Heat capacity of block copolymers of styrene (S) and α-methyl styrene (MS). Successive curves are shifted upwards by 40 J/(K mol).

*A microphase has phase dimensions of less than one micrometer.

higher transition temperature of the second component. The reverse is true at the upper glass transition. Here the interface is made to the already liquid polystyrene and the asymmetric broadening goes to the low-temperature side. The degree of broadening can even be calibrated with an approximate structure parameter. The top DSC traces in Fig. 24 show a substantial amount of broadening for three di- and tri-block copolymers. The overall mass percentage of α-methyl styrene is given in parentheses next to the sample abbreviation in the figure.

In blends, such asymmetric broadening is expected only on quenching to an unstable dispersion of phase regions of small sizes. Compatible blends of homopolymers show also some broadening of the glass transition when compared to the homopolymer. The reason for this latter broadening must lie in the mixing that is limited in polymers to the neighbors next to the chain. No mixing can occur along the chain. There a noticeable broadening, even if the second component is a low molecular mass component.

In semicrystalline polymers the crystals are separated into microphases. In Fig. 20 it is shown that, similar to block copolymers, this can cause extreme broadening of the glass transition. In addition, it can lead to an outright increase in the glass transition, as is shown in Fig. 25. Here data are given for poly(oxy-1,4-phenyleneoxy-1,4-phenylene-carbonyl-1,4-phenylene) (PEEK).[24] The glass transition temperature of quenched, fully amorphous PEEK is 419 K. On fast crystallization at a low temperature, T_c, the glass transition is not only broadened, but also raised to 430 K. As higher crystallization temperatures are chosen, the interface is less strained and T_g decreases as shown in the graph.

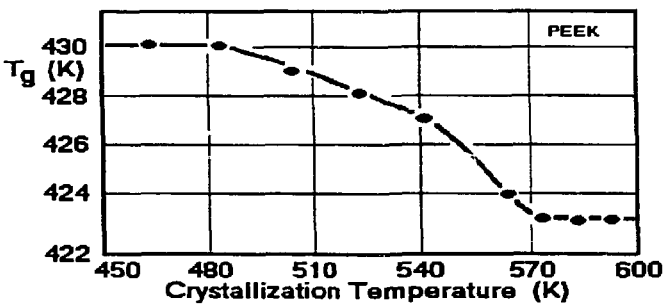

Fig. 25. Relationship between the glass transition temperatur of PEEK and the isothermal crystallization temperature.

In addition to these shifts in T_g and broadening, a quantitative analysis of ΔC_p shows that there is a decrease in ΔC_p beyond that expected from the crystalline content. Since it was proposed above that ΔC_p is a characteristic constant for any given material, this decrease in C_p must be an indication that some of the amorphous part is hindered to such a degree that is *rigid*, i.e. it possesses the lower heat capacity of the glass instead of the higher heat capacity of the liquid. Figure 26 illustrates the change of the rigid amorphous fraction with cooling rate for semicrystalline poly(thio-1,4-phenylene), poly(phenylene sulfide) or PPS.[25] The abscissa of the plot is given in terms of the natural logarithm. On fast cooling, the crystals are poor and have a very large surface area. These are the conditions to produce a large fraction of rigid amorphous polymer. On slow cooling, the rigid amorphous fraction decreases.

For each individual polymer the conditions and amount of rigid amorphous fraction seems to be different. For poly(oxy-2,6-dimethyl-1,4-phenylene)[26] and poly(butylene terephthalate),[27] for example, the rigid amorphous fraction can be practically 100%, while for more mobile molecules, such as poly(ethylene oxide) the interaction between crystal and amorphous fraction seems to produce only a moderate upward shift in T_g without effect on ΔC_p. Again, this characterization, important for the industrial application of macromolecules materials, can best be carried out by advanced thermal analysis, *ATHAS*.

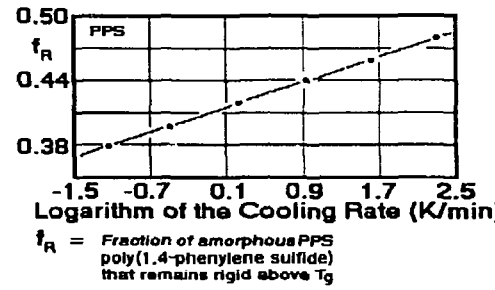

Fig. 26. Rigid amorphous fraction above the glass transition temperature in poly(1,4-phenylene sulfide).

Acknowledgments

This work was supported by the Division of Materials Research, National Science Foundation, Polymers Program, present Grant # DMR 8818412, and the Division of Materials Sciences, Office of Basic Energy Sciences, U.S. Department of Energy, under Contract DE-AC05-84OR21400 with Martin Marietta Energy Systems, Inc.

References

1. B. Wunderlich and S. Z. D. Cheng, *Gazetta Chimica Italiana*, 116, 345 (1986).

2. *ATHAS* data bank, updated every 6 months, request copy from the author. For the data bank of experimental heat capacities see: U. Gaur, S.-F. Lau, H.-C. Shu, B. B. Wunderlich, M. Varma-Nair, and B. Wunderlich, *J. Phys. Chem. Ref. Data*, 10, 89, 119, 1001, 1051 (1981); 11, 313, 1065 (1982); 12, 29, 65, 91 (1983); and (1990), to be published.

3. P. Debye, *Ann. Physik*, 39, 789 (1912).

The one-dimensional Debye function is:

$$D_1(\Theta/T_1) = (T/\Theta_1) \int_0^{(\Theta/T_1)} [(\Theta/T)^2 \exp(\Theta/T)]/[\exp(\Theta/T) - 1]^2 d(\Theta/T) \qquad \Theta = h\nu/k$$

For tables of the one-dimensional Debye Function see:
B. Wunderlich, *J. Chem. Phys.*, *37*, 1207 (1962).

The two-dimensional Debye function is:

$$D_2(\Theta/T_2) = 2(T/\Theta_2)^2 \int_0^{(\Theta/T_2)} [(\Theta/T)^3 \exp(\Theta/T)]/[\exp(\Theta/T) - 1]^2 d(\Theta/T)$$

For tables of the two-dimensional Debye Function see:
U. Gaur, G. Pultz, H. Wiedemeier and B. Wunderlich, *J. Thermal Anal.*, 21, 309 (1981).

The three-dimensional Debye function is:

$$D_3(\Theta/T_3) = 3(T/\Theta_3)^3 \int_0^{(\Theta/T_3)} [(\Theta/T)^4 \exp(\Theta/T)]/[\exp(\Theta/T) - 1]^2 d(\Theta/T)$$

For tables of the the three-dimensional Debye Function see:
J. A. Beatty, *J. Math. Phys. (MIT)*, **6,1** (1926/27).

For computer programs and a general discussion of the functions see: Yu. V. Cheban, S. F. Lau and B. Wunderlich, *Colloid Polymer Sci.*, **260**, 9 (1982).

4. A. Einstein, *Ann. Physik*, 22, 180, 800 (1907).

The Einstein function is:

$$E(\Theta/T_E) = [(\Theta/T)^2 \exp(\Theta/T)]/[\exp(\Theta/T) - 1]^2 \qquad \Theta = h\nu/k$$

Tables of the Einstein Function can be found, for example, in J. Sherman and R. B. Ewell, *J. Phys. Chem.*, **46**, 641 (1942); D. R. Stull and F. D. Mayfield, *Ind. Eng. Chem.*, **35**, 639 (1943); J. Hilsenrath and G. G. Ziegler, "Tables of Einstein Functions," *Natl. Bur. Stands. Monograph*, **49** (1962). By now, any good pocket calculator is, however, able to give 10 digit precision with programmed calculation within a fraction of a second.

5. A detailed discussion of the match of heat capacities and the low-frequency vibrational spectrum is given by: H. S. Bu, S. Z. D. Cheng and B. Wunderlich, *J. Phys. Chem.*, 91, 4179 (1987).

6. R. Pan, M. Varma, and B. Wunderlich, *J. Thermal Anal.*, **35**, 955 (1989).

A universal approximation was shown to be:

$C_p - C_v = 3RA_oC_pT/T_m^\circ$ with T_m° representing the melting temperature, and $A_o = 3.9\times10^{-3}$ (K mol)/J.

7. J. Grebowicz, H. Suzuki and B. Wunderlich, *Polymer*, **26**, 561 (1985).

8. V. V. Tarasov, *Zh. Fiz. Khim.*, 24, 111, (1950); **27**, 1430 (1953); see also: *ibid.* 39, 2077 (1965); *Dokl. Akad. Nauk SSSR*, **100**, 307 (1955).

9. S.-F. Lau and B. Wunderlich, *J. Thermal Anal.*, **28**, 59 (1983).

10. U. Gaur, M.-Y. Cao, R. Pan and B. Wunderlich, *J. Thermal Anal.*, 31, 421 (1986).

11. R. Pan, M.-Y. Cao and B. Wunderlich, *J. Thermal Anal.*, 31, 1319 (1986).

12. For a description of the theory of heat capacities of liquid macromolecules see: K. Loufakis and B. Wunderlich, *J. Phys. Chem.*, **92**, 4205 (1988).

13. H. Suzuki and B. Wunderlich, *J. Polymer Sci., Polymer Phys. Ed.*, **23**, 1671 (1985).

14. S. F. Lau, H. Suzuki and B. Wunderlich, *J. Polymer Sci., Polymer Phys. Ed.*, **22**, 379 (1984).

15. K. Loufakis and B. Wunderlich, *J. Polymer Sci., Polymer Phys. Ed.*, **25**, 2345 (1987).

16. B. Wunderlich and J. Grebowicz, *Adv. Polymer Sci.*, **60/61**, 1 (1984).

17. M.-Y. Cao and B. Wunderlich, *J. Polymer Sci., Polymer Phys. Ed.*, **23**, 521 (1985). For an update see *Polymers for Advanced Technology* Vol. 1 (1990).

18. B. Wunderlich and L. D. Jones, *J. Macromol. Sci.*, **B3**, 67 (1969).

19. B. Wunderlich, *J. Polymer Sci., Part C*, **1**, 41 (1963).

20. H.-C. Shu, U. Gaur and B. Wunderlich, *J. Poly. Sci., Polymer Phys. Ed.*, **18**, 449 (1980).

21. J. Grebowicz, W. Aycock and B. Wunderlich, *Polymer*, **27**, 575 (1986).

22. B. Wunderlich, M. Möller, J. Grebowicz and H. Baur, "Conformational Motion and Disorder in Low and High Molecular Mass Crystals." Springer Verlag, Berlin, 1988, (*Adv. Polymer Sci.*, Vol. **87**).

23. U. Gaur and B. Wunderlich, *Macromolecules*, **13** 1618 (1980).

24. S. Z. D. Cheng and B. Wunderlich, *Macromolecules*, **19**, 1868 (1986).

25. S. Z. D. Cheng and B. Wunderlich, *Macromolecules*, **20**, 2801 (1987).

26. S. Z. D. Cheng and B. Wunderlich, *Macromolecules*, **20**, 1630 (1987).

27. S. Z. D. Cheng and B. Wunderlich, *Makromol. Chemie*, **189**, 2443 (1988).